LUND UNIVERSITY

PHYSICS OF LOW-DIMENSIONAL STRUCTURES AND QUANTUM DEVICES

FFFN35

DECEMBER 18, 2019

Coulomb Blockade with Rate Equations

Authors:
André ANDERSEN
Oskar ANDERSSON
Daniel LE

Instructor:
Martin JOSEFSSON

1 Introduction

In this project the current and the conductance seen in the Coulomb Blockade lab (for a quantum dot) will be solved numerically. Furthermore, a stability diagram for the device will be generated by focusing on the regime of small tunnel couplings, where electrons tunnel through the device one by one. This means the mathematics become rather simple.

However, it is required to solve the so-called rate equations in order to obtain the correct IV-characteristics. The solutions to the rate equations will yield the occupation probabilities of the many-body states of the device, from which the current can be obtained.

2 Theory

The quantum dot is modelled as having few states whilst strong Coulomb interactions are present. This limitation makes the simulation of the quantum dot simpler. Thus, the theory derived next is therefore based on this limitation. However, that is not to say it is a bad model. This model is in fact used to describe the single electron transistor and is a versatile tool used in quantum transport research to investigate e.g heat engine quantum dots [1] and architectures for quantum computing [2].

2.1 The states and energies of a quantum dot

A quantum dot can be described as an artificial atom, and similarly to an atom, a quantum dot has several states. The energies, $E_i(N)$ of these so called *many-body states*, $|N, i\rangle$, is used to characterize the quantum dot, where the index i describes the different many-body states with N electrons [3].

As the device is small, the electrons will interact with each-other with Coulomb interactions. Hence, the total energy is modelled by the so called *constant interaction model* [4]. It is given by following equation

$$E_{tot} = \sum_{i}^{N} E_i(N) = U(N) + \sum_{k \in \Omega_i}^{N} \epsilon_k, \tag{1}$$

where *U(N)* is defined as the energy stored electrostatically in this system and ϵ_k is defined as the energies of the occupied single-particle orbitals in the state i, Ω_i. When defining the orbital index i, spin degeneracy is taken into consideration. In the absence of a magnetic field, two occupied single-particle orbitals in the same state will have the same energy [3].

The energies can be used to define the chemical potential of the dot by:

$$\mu_N^{ij} = E_i(N) - E_j(N-1). \tag{2}$$

Given the chemical potentials of the dot, it is possible to obtain the regions where the current is zero. Furthermore, if the tunnel couplings are known, the current can be numerically solved as a function of gate voltage, i.e a stability diagram can be modelled [3].

2.2 Tunnel rates

The state of the quantum dot is varying as electrons tunnels on and off the dot. A probability, P_{Ni} for being in the state $|N, i\rangle$ can be obtained by solving the so called *rate equations*. To solve the rate equations it is required to determine the *tunnel rates* first. When an electron tunnels into a quantum dot in the initial state $|N-1, j\rangle$, the dot will have its state altered to $|N, i\rangle$. The total rate for this tunneling process is described by [3]

$$W_{Ni,(N-1)j} = \sum_{r=L,R} \Gamma^r_{Ni,(N-1)j} \cdot f_r(\mu_N^{ij}) \tag{3}$$

where $\Gamma^r_{Ni,(N-1)j}$ is the tunnel coupling between the quantum dot and either its left lead (r = L) or its right lead (r = R). A tunnelling process can only occur if there is an available electron on one of the leads, which is why the Fermi-Dirac distribution, $f_r(\epsilon^{ij})$ is included in equation 3 [3]. This distribution is given by [5]

$$f(\epsilon) = \frac{1}{e^{(\mu_N - \mu_r)/k_b T} + 1} \tag{4}$$

where μ_N is the energy input, μ_r is the chemical potential of either the right or left lead and k_b is the Boltzmann constant. It is clear that since the state occupancy of the quantum dot depends on the Fermi-Dirac distribution, it will also be temperature dependant.

In contrast, an electron that tunnels out of the quantum dot changes the initial state of the dot, $|N+1, j\rangle$ to $|N, i\rangle$. This process is then given by

$$W_{Ni,(N+1)j} = \sum_{r=L,R} \Gamma^r_{Ni,(N+1)j} \cdot \left(1 - f_r(\mu_{N+1}^{ij})\right) \tag{5}$$

When an electron tunnels out of the dot, an empty state is needed in one of the electrodes, which is evident in the second term in 5, i.e one minus the Fermi-Dirac distribution [3].

2.3 Rate equations

The probability of a state, $|N, i\rangle$ being occupied is given by $\boldsymbol{P}_{Ni}$. Thus, the derivative of the probability with respect to time, $\dot{\mathbf{P}}_{Ni}$ is a sum of all the tunnel rates associated with the occupation of a state $|N, i\rangle$, minus the tunnel rates associated with the depopulation of a state $|N, i\rangle$, and is given by

$$\dot{\mathbf{P}}_{Ni} = \sum_{N'=N\pm1} \sum_j W_{Ni,N'j} \cdot P_{N'j} - \sum_{N'=N\pm1} \sum_j W_{N'j,Ni} \cdot P_{Ni} \tag{6}$$

where $P_{N'j}$ and P_{Ni} are the weighted probabilities for the processes leading to an occupation of a state and a depopulation of a state, respectively [3].

Assuming steady state, $\dot{\mathbf{P}}_{Ni}$ can be set to zero. This generates a set of linear equations and can be solved to obtain all occupation probabilities during a long time, given the probability normalization $\sum_{Ni} P_{Ni} = 1$. Thus, stationary properties like current can be acquired from this result. With the occupation probabilities, this is done by counting the amount of electrons tunneling out of the electrode r, and subtracting the electrons tunneling in. This calculation is weighted by a probability of the dot being in the analogous initial state. The equation for the current is as follows [3]:

$$I_{QD} = I_r = -e \sum_N \sum_i \sum_{N'=N\pm1} \sum_j W^{I_r}_{Ni,N'j} \cdot P_{N'j} \tag{7}$$

where

$$W^{I_r}_{Ni,(N-1)j} = \Gamma^r_{Ni,(N-1)j} \cdot f_r(\mu^{ij}_N) \tag{8}$$

which signifies the tunnel rate of depopulation of a state and

$$W^{I_r}_{Ni,(N+1)j} = -\Gamma^r_{Ni,(N+1)j} \cdot \Big(1 - f_r(\mu^{ji}_{N+1})\Big) \tag{9}$$

which signifies the tunnel rate of occupation of a state.

2.4 The effect of an external magnetic field: Zeeman splitting

Assuming no external magnetic field is applied, the single-particle orbital is spin degenerate, with the energies ϵ_1 and ϵ_2, which are the same. In the presence of an external magnetic field, these states will split because of magnetic-spin interactions in the quantum dot. This is called the Zeeman effect and only strong magnetic fields are considered as otherwise it would complicate the model used considerably (to avoid effects such as *Russell–Saunders coupling*) [6]. The energy split of the states, $\epsilon^{'}_B$, can be written as [7],[8]

$$\epsilon^{'}_B = g\mu_B B \tag{10}$$

where g is the *Landé g-factor* , μ_B is the Bohr magneton, and B is the applied magnetic field in the order of $\sim$ 1 T. This energy will be added to the system described by equation 1 & 2. The g-factor is a material property that describes the angular and magnetic momenta of a particle and for an electron in vacuum $g \approx 2.00232$.

3 Results and discussion

The values used for this experiment is $\Gamma = 1$ GHz (it is assumed the barriers are equal; this value was chosen arbitrarily, but is a possible tunneling rate [9]), $C_\Sigma = 10^{16}$, $\alpha_g = 0.1$, $E_C = e^2/C_\Sigma$ (This is the energy from the capacitive coupling preventing the electrons from simply entering the quantum dot), $\mu_B = 9.274 \cdot 10^{-24}$ and $g = 3$ (This corresponds to the g-factor for p-type GaSb used in the Coulomb Blockade lab [8]).

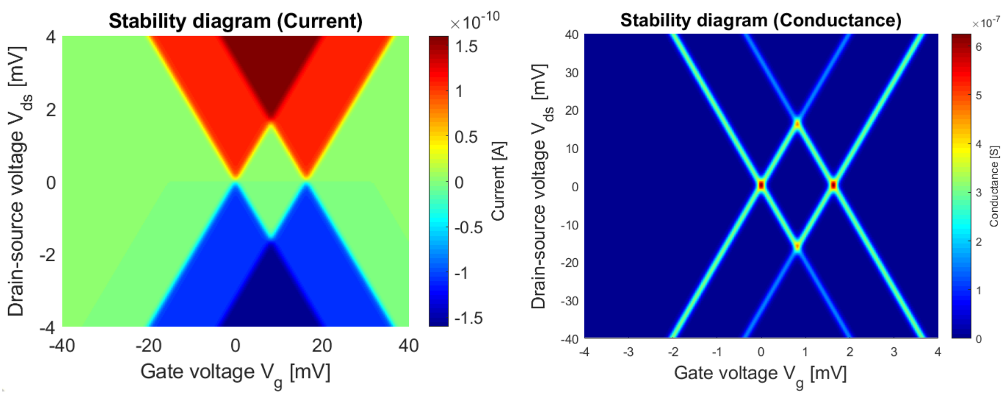

Figure 1: The current and conductance at $T = 1$ K and $B = 0$ T. In the first part, the pairs of triangles produced by the two non-degenerate energy levels in the quantum dot can be seen. The second part shows the conductance of the quantum dot, which is related to dI/dV_{ds}. As V_g is swept the conductance lines show values where there are charge carriers traveling through the barriers and at the intersections (which are proportional to the charging energy) there will be local maximums in conductance.

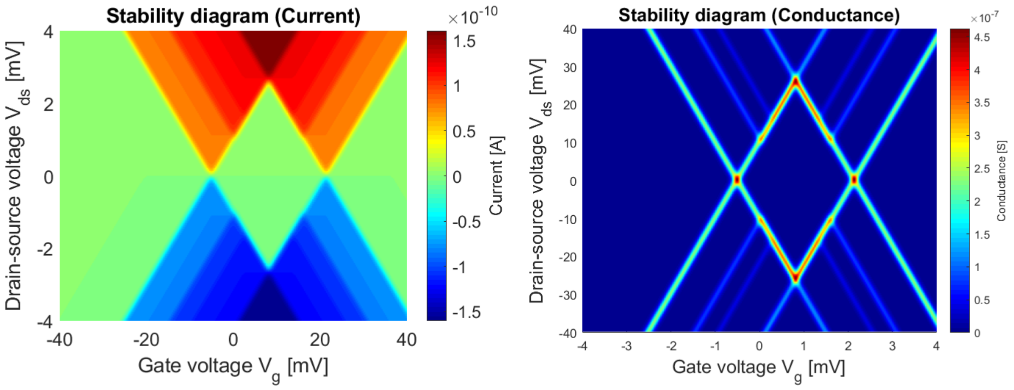

Figure 2: Now a magnetic field is applied. The current and conductance is shown for $T = 1$ K and $B = 3$ T. Since the two single electron states are no longer degenerate, the triangle pairs and conductance lines are split into more levels. Notice that the diamond now is larger because there is more states for the electrons to tunnel through while the maximum conductance has decreased since the Γ and the barrier of entry stay the same.

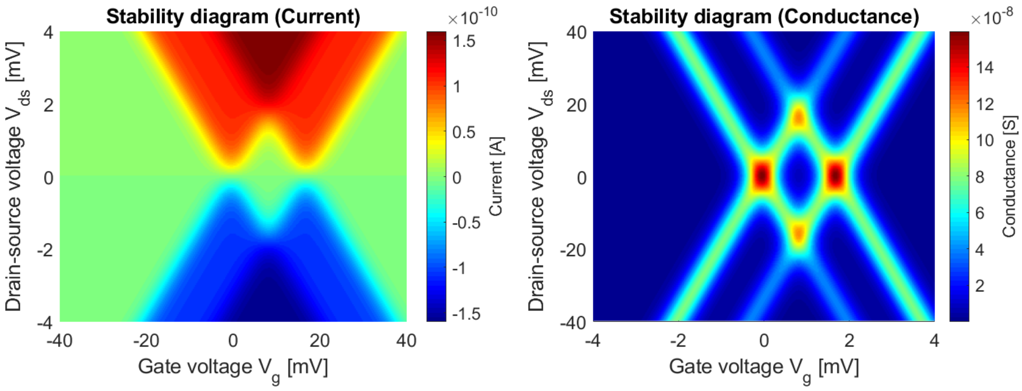

Figure 3: Here the temperature has been increased while the magnetic field is once again set to zero. It shows the current and conductance at $T = 3$ K. Notice that the current and conductance lines are more diffuse which is caused by the more "smeared" Fermi-Dirac distribution.

In this simulation project, the current through the quantum dot is generated by sweeping both V_{SD} and V_G. However, it is also possible to generate current by utilizing temperature gradients. This is apparent when observing equation 4; the quantum dot current is dependent on temperature. Thus, the Fermi-Dirac distribution can be manipulated by altering the temperature. This is of importance because by heating one of the leads and keeping the other one cold the Fermi-Dirac distributions of the leads will appear as seen in the figure below

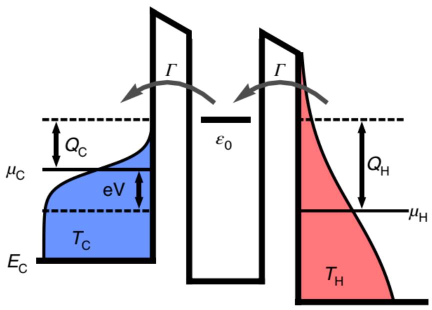

Figure 4: Illustration of the band diagram of a quantum dot that functions as a heat engine. The dot is coupled to hot and cold electron reservoirs where the Fermi-Dirac distributions are described by temperatures and chemical potentials T_H, μ_H and T_C, μ_C, respectively. γ is still equal for left and right barrier while E_C indicates the band energy of the cold side (blue) instead of the charging energy. Q_C and Q_H indicates the charge stored above the chemical potentials due to the difference in temperature. ϵ_0 indicates a state in the quantum dot [1].

As V_G is swept, electrons from the hot electron reservoir will tunnel to the cold reservoir as the Fermi-Dirac distribution has more thermal broadening in the hot reservoir. Consequently, if there is a flow of charge carriers from lower to higher potential, (as indicated by the band structure in figure 4) thermal energy is converted into electrical energy. At lower energies, more electrons are accumulated up to the chemical potential in the cold reservoir. Thus, as V_G is swept further, the energy level inside the quantum well will sink until electrons will start to tunnel from the cold reservoir to the hot reservoir. The heat engine will therefore only consume energy.

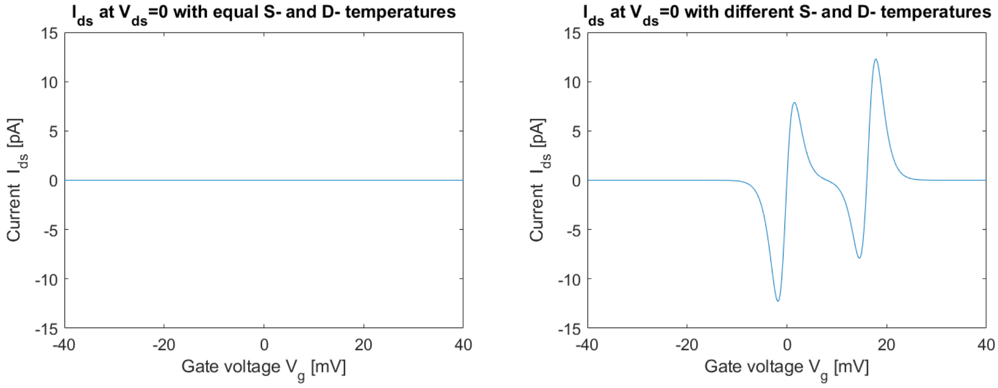

Figure 5: Current versus gate voltage in a quantum dot heat engine when source-drain voltage is 0 V. In the left figure the temperatures on the electron reservoirs (source and drain) are the same. In the right figure the temperatures on the electron reservoirs are different ($T_L = 1K$ & $T_R = 1.5K$).

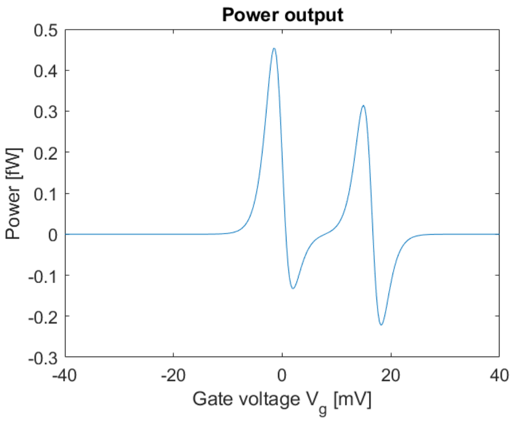

Figure 6: The power output of the device for a small source-drain bias with temperatures T_L = 1 K & T_R = 1.5 K

In order to prove the concept, a bias can be applied across the quantum dot when the temperatures on each lead is different. When the dot is in a conducting state under these conditions, power is generated similarly to when a current runs through a resistor. This is shown in figure 6. This also means there is a resemblance between the IV-characteristics in a functioning heat engine quantum dot and the power output of a resistor. This is because the electrical power is directly proportional to the current and resistance.

References

[1] Martin Josefsson et al. A quantum-dot heat engine operating close to the thermodynamic efficiency limits. *Nature Nanotechnology*, 13, October 2018.

[2] Kuei-Lin Chiu. Single electron transport and possible quantum computing in 2d materials. *Key Laboratory of Quantum Information, University of Science and Technology of China*, April 2018.

[3] *Coulomb blockade with rate equations - Manual.* 2019.

[4] Coulomb blockade in quantum dots. `http://www.ftf.lth.se/fileadmin/ftf/Course_pages/FFF042/cb_lecture07.pdf`. Accessed: 2019-12-13.

[5] John H Davies. *The physics of low-dimensional semiconductors.* 6th edition, 1998.

[6] Ruslan P. Ozerov and Anatoli A. Vorobyev. *Physics for Chemists.* 2007.

[7] Edgar Bonet et al. Solving rate equations for electron tunneling via discrete quantum states. *Physical review B*, 65, 2002.

[8] Xiaoyang Mu, Gerard Sullivan, and Rui-Rui Du. Effective g-factors of carriers in inverted inas/gasb bilayers. *Appl. Phys. Lett.*, 108, 2016.

[9] Alessandro Andreev A. Kodera T. Kambara T. Lin W. Oda Shunri Williams David. Ferrus, T. Rossi. Ghz photon-activated hopping between localized states in a silicon quantum dot. *New Journal of Physics*, 16, 2013.